◉ 速報硏究論文

# Flows Characteristics of Developing Turbulent Pulsating Flows in a Curved Square Duct

G. M. Park* · T. G. Bong** · H. C. Son***

# 곡관덕트내의 입구영역에서 난류 맥동유동의 유동특성

박길문 · 봉태근 · 손현철

## Abstract

In this study, the flow characteristics of developing turbulent pulsating flows in a square-sectional 180° curved duct are investigated experimentally. The experimental study of air flow in a square-sectional curved duct is carried out to measure axial velocity distribution, secondary flow velocity profiles and wall shear stress distributions by using a Laser Doppler Velocimetry system with the data acquisition and processing system of Rotating Machinery Resolver (RMR) and PHASE software, at the entrance region of the duct which is divided into 7 sections from the inlet($\phi=0°$) to the outlet ($\phi=180°$) in 30° intervals.

The results obtained from the study are summarized as follows :

(1) The time-averaged critical Dean number of turbulent pulsating flow ($De_{ta,cr}$) is greater than $75\omega^{+}$. It is understood that the critical Dean number and the critical Reynolds number are related to the dimensionless angular frequency in a curved duct.

(2) Axial velocity profiles of turbulent pulsating flows are of an annular type, similar to those of turbulent steady flows.

(3) Secondary flows of turbulent pulsating flows are strong and complex at the entrance region. As velocity amplitudes ($A_1$) become larger, secondary flows become stronger.

(4) Wall shear stress distributions of turbulent pulsating flows in a square-sectional 180° curved duct are exposed variously in the outer wall and are stabilized in the inner wall without regard to the phase angle.

* Chosun University(receipt : '99. 4.)
* * Mokpo Maritime Unive)
* * * Gradurate School of Chosun Univ.)

## Introduction

With the progress of industrial development, all sorts of pipe network systems have become gradually greater and more complex state. In addition, the design of the pipe network is closely connected with both the stability and efficiency of entire plant.

In the 1940' s, studies were made on constraint breach boilers and chemical reactors. In the 1950' s, they included studies on flows with a large bended angle-high Dean Number-related to a heat exchanger such as a cooling system in an atomic power plant. Since the 1970' s, studies of unsteady flows have been based on the development of the analysis and experimental method.

In recent years, the effects of secondary flows in the bend part of a lung-airway are connected with the field of bio-medical engineering relating to the transfer of oxygen and carbonic acid gas, one of the most important functions in blood, and gas exchange by convection and diffusion in the lungs.

The history of studies of unsteady flows in curved ducts is not long, most of the researches having been conducted since 1970.

Studies of fluid flows in curved ducts started in the late 19th century. In 1910, Eustice[1] suggested that the change from a straight-duct flow to a coiled-duct flow was accompanied by an increased resistance. In 1927, Dean[2] classified a flow into two different types : the main flow, which is in the axial direction, and the secondary flow which is perpendicular to the axial direction. He suggested that the flow in the curved duct depends on a specified parameter, that is the Dean number $De(=Re\sqrt{a/R}=Re\sqrt{D_h/2R})$.

As for studies of oscillatory flow, Lyne[3] theorized that the secondary flow is governed by the Reynolds number, developing asymptotic theories for both small and large values of this parameter. Studies on axial velocity have found that secondary flow is generated from the outer wall to the inner wall, the so-called Lyne' s secondary flow.

Zalosh et.al.[4] indicate through an experiment that a flow field of small dimensionless angular frequency ($\omega^+$) is similar to a steady flow configuration of low Dean number, whereas a flow field of large dimensionless angular frequency ($\omega^+$) includes a secondary flow directed towards the center of curvature.

Mullin[5] conducted a theoretical and experimental study of oscillatory flow in a curved duct, in which he identified that the equation for fully developed laminar flow depends on the amplitude parameter and the frequency parameter.

A pulsating flow is one in which steady flow is supplemented by an oscillatory flow. For pulsating flow, Smith[6] made a theoretical study of the entrance region, while Singh[7] found that the pressure distribution is not significantly influenced by secondary flow during the initial development of motion. Singh et. al.[8] suggested that the increase of the secondary flow caused by the curvature draws off the slower moving fluid azimuthally from the outer bend to the inner bend.

Talbot et. al.[9] conducted two experiments by using parameters $Rc=1/20$, $1/7$, $\omega^+=8.0$, $12.5$, and $De=120$, $372$ and reporting the flow characteristics. Kita et. al.[10] experiment shows that fluctuation of the boundary layer grows on the end plate of the duct. Naruse et. al.[11] measured the developing pulsating flow in order to determine the characteristics of blood flow in a strongly curved duct, that is, the internal carotid artery called the siphon portion.

In this study, the critical Dean number of turbulent pulsating flows is determined in a square-sectional curved duct. It was found that the dimensionless angular frequency ($\omega^+$), the Dean number (De) and the velocity amplitude ratio ($A_1$) affected the characteristics of secondary flow and examined the wall shear stress distribution.

## 2. Experimental Procedures

### 2.1 Experimental Apparatus

In order to conduct the experiment, a square-sectional 180° curved duct was used. As a duct of 40×40mm, the inlet straight duct had a length of 4000mm and included a rectify box and an inlet bell mouth in the entrance of the duct. The outlet straight duct was equal to the inlet straight duct.

A pulsating is an oscillatory flow which is operated by a Scotch-yoke type oscillator superimposed on a steady flow made by a blower.

The LDV power source was an Ar-ion laser with a maximum output of 2Watt and including a dual-beam type of 2 colors and 3 beams and a back-scattered type. The experimental apparatus was attached to a three-dimensional traverse which could move and load the LDV system to measuring the velocity distribution in the test duct.

The Rotating Machinery Resolver was used

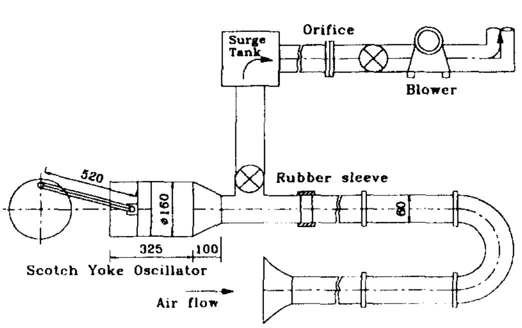


**Fig. 1 Schematic diagram of experimental apparatus**

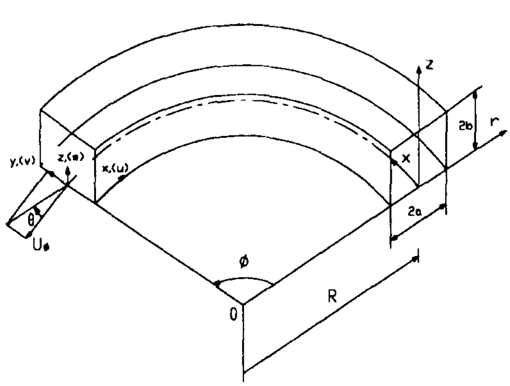


**Fig. 2 Coordinate system of curved duct apparatus**

to calculate the axial velocity, secondary flow and wall shear stress distributions of the turbulent pulsating flow. An encoder was connected to the rotating axis of a variable-speed motor. Fig. 1 shows the design drawing and structure of the Scotch-yoke type oscillator. Fig. 2 shows the coordinate system of the curved duct apparatus.

### 2.2 Experimental Method

A pulsating flow is an oscillatory flow which is operated by a Scotch-yoke type oscillator superimposed on a steady flow made by a blower. Therefore the velocity control of the steady flow was attained by a flow rate control valve set up between the surge tank and the blower.

For oscillatory flows, the frequency (f) was controlled by the variable motor of the Scotch-yoke type oscillator, and the piston amplitude ($A_p$) was controlled by controlling the positions of the crank plate.

First the velocity waveforms were recorded on a photocorder at the center of the 150° of bend at which are believed to develop at the flow region.

A signal was received from the sensor of a hot-wire anemometer which was inserted at the center region of the curved duct. A signal

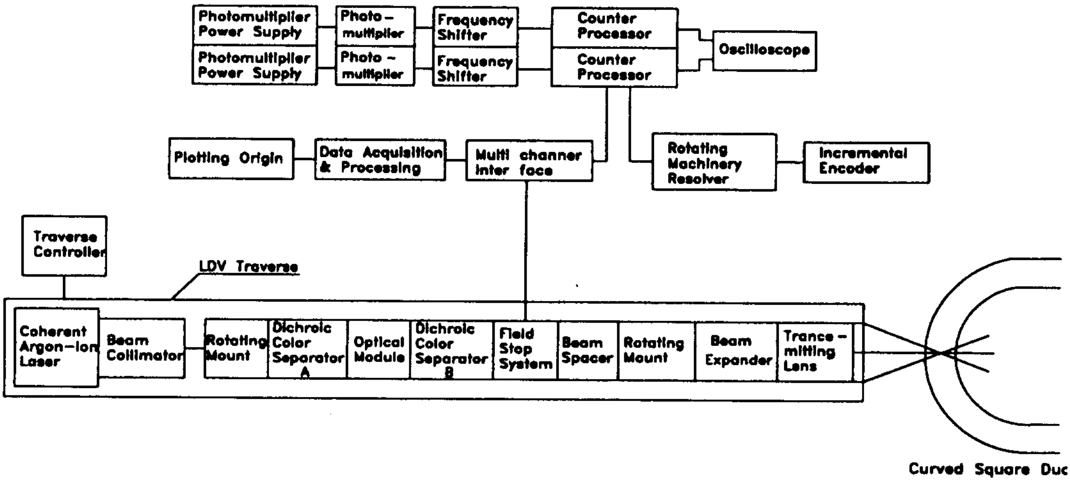


**Fig. 3 Schematic diagram of LDV system**

**Table 1. Experimental conditions of turbulent pulsating flow**

| Angle | f(Hz) | R(mm) | $\omega^+$ | Ap(mm) | $De_{os}$ | $De_{ta}$ | $A_1$ |
|---|---|---|---|---|---|---|---|
| 0° | 2.0 | 400 | 18.2 | 50 | 705 | 780 | 0.9 |
| | | | | | | 990 | 0.7 |
| 30° | 2.0 | 400 | 18.2 | 50 | 705 | 780 | 0.9 |
| | | | | | | 990 | 0.7 |
| 60° | 2.0 | 400 | 18.2 | 50 | 705 | 780 | 0.9 |
| | | | | | | 990 | 0.7 |
| 90o | 2.0 | 400 | 18.2 | 50 | 705 | 780 | 0.9 |
| | | | | | | 990 | 0.7 |
| 120° | 2.0 | 400 | 18.2 | 50 | 705 | 780 | 0.9 |
| | | | | | | 990 | 0.7 |
| 150° | 2.0 | 400 | 18.2 | 50 | 705 | 780 | 0.9 |
| | | | | | | 990 | 0.7 |
| 180° | 2.0 | 400 | 18.2 | 50 | 705 | 780 | 0.9 |
| | | | | | | 990 | 0.7 |

was analyzed through the photocorder from laminar flow to turbulent pulsating flow. An experiment was conducted at the region where an initial turbulent burst was about to develop.

When the angular frequency of oscillation was 2Hz, the piston amplitude was 50mm. When the oscillatory Dean number was 705, the time-averaged Dean number changed from 780 to 990 respectively. Scattered particles formed a mosquito smoke of 0.1∼0.3 diameter.

Measurements for the turbulent pulsating flows were taken over 30° intervals at 0°, 30°, 60°, 90°, 120°, 150°, and 180° in the curved duct by using the LDV system and LDV traverse system, and then make flow analysis is made these measurements of pulsating flow are performed by using the LDV system with an encoder and RMR.

Measurement positions included 15 in the y*-direction and 7 in the z*-direction. Experimental data were obtained through a data acquisition & processing system. The data were processed with PHASE software and plotted with Origin Graphic software, as shown in Fig. 3.

Table 1 gives the list of the experimental conditions for developing turbulent pulsating flows.

## 3. Results and Considerations

### 3.1 The classification of flow regions

As the turbulent pulsating flow progresses downstream from the entrance region of the duct, the boundary layer develops gradually under viscosity action, becoming a fully developed flow region. The critical Dean number of

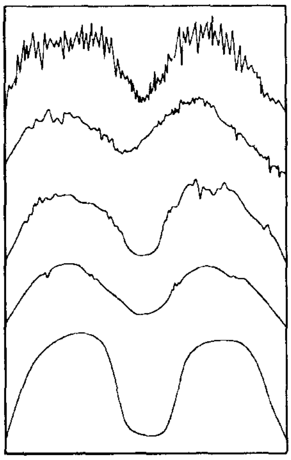


**Fig. 4 Waveforms of pulsating flow in the curved duct from the hot-wire anemometer**

the pulsating flow is calculated by using the time-averaged cross-sectional mean velocity as follows :

$$De_{ta,cr}=\left(\frac{u_{m,ta}\cdot D_h}{\nu}\right)\sqrt{D_h/2R} \quad (1)$$

The ratio of curvature radius (Rc), time-averaged Dean number ($Re_{ta}\sqrt{(D_h/2R)}$), dimensionless angular frequency($\omega^+$), and velocity amplitude ratio ($A_1$) have an influence on the flow, but the characteristics of the pulsating flow were mainly governed by the time-averaged Dean number($Re_{ta}\sqrt{(D_h/2R)}$), dimensionless angular frequency($\omega^+$) and velocity amplitude ratio ($A_1$) under the conditions of this experiment. Fig. 4 shows the hot-wire anemometer and velocity waveforms from the photocorder, which classifies the flow region of turbulent pulsating flows.

### 3.2 Axial direction velocity profiles

As in Fig. 5, the dimensionless angular frequency($\omega^+$) is 18.2, the time-averaged Dean number ($De_{ta}$)=990 and the velocity amplitude ratio($A_1$) is 0.7. Because of the effect of the steady ingredient, the axial velocity distribution shows velocity distribution profiles similar to those for steady flow.

In the concave phenomenon of the duct center, if the Dean number is large, a maximum value of centrifugal force is generated at the second part of the inner wall and outer wall. However, an additional vortex is extinguished because the axial velocity distribution is flat according to the acceleration of the developing phase and duct center fluid. If the time-averaged Dean number ($De_{ta}$) increases, the convex part of the duct center becomes a distribution type similar to symmetry.

Covering the total phase and passing the point of the bend angle 30°, the axial velocity distribution becomes an annular type because the inertia force increases relatively in comparison with the viscosity force of the wall. The inner and outer velocity gradient of the curved duct is comparatively slow and the velocity change is small. Also, because of the same-size centrifugal force during one cycle, it becomes a large axial-velocity type at the outer wall, as well as becoming a developing flow of the curved duct.

The velocity distribution of pulsating flow according to the dimensionless cross section position of the duct is shown to be a concave type because the phase delay and $|u_{os,1}|$ distribution are relatively larger at the central region of the duct than at the inner region. It shows an annular type from the bend angle 30°. The above statements are known to agree with the experimental results of Austin[13].

Some of the important dimensionless variables-the ratio of curvature radius (Rc), the time-averaged Dean number ($Re_{ta}\sqrt{(D_h/2R)}$), the dimensionless angular frequency($\omega^+$), the velocity amplitude ratio ($A_1$), etc-have great effect on the flow, but the ratio of curvature radius (Rc) has not effect on the flow. Accord-

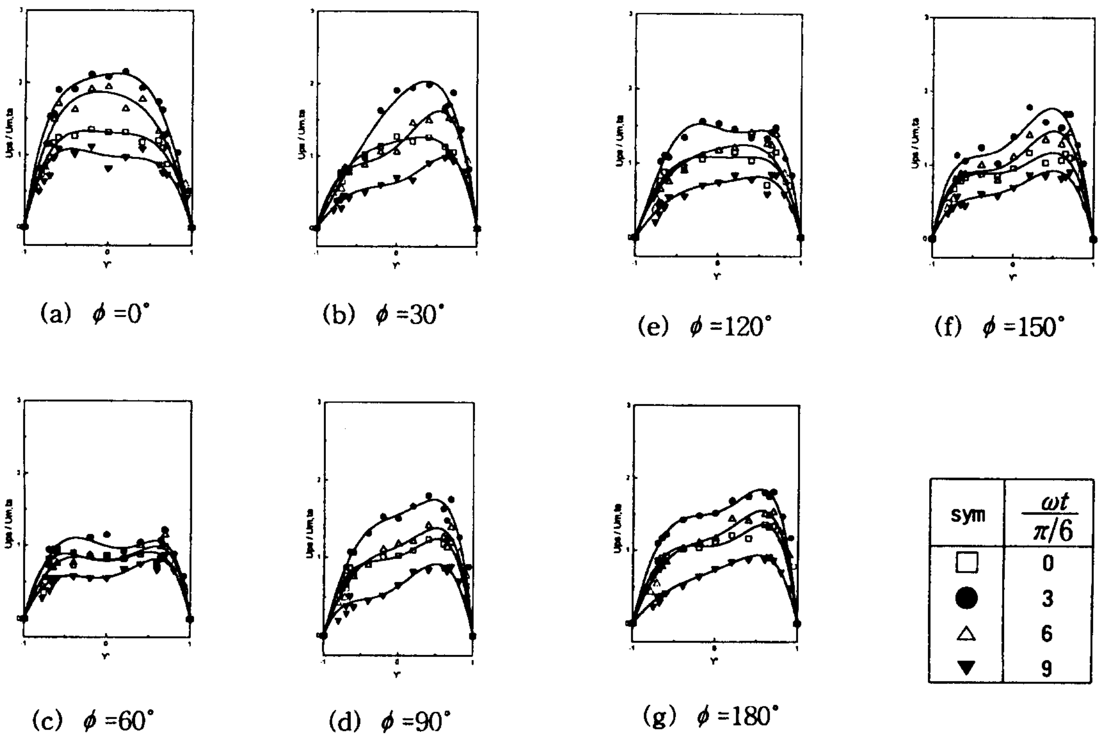


**Fig. 5 Axial velocity distributions along the y* variation in a curved duct for turbulent pulsating flow at $De_{ta}=990$, $\omega^+=18.2$, $A_1=0.7$.**

ingly, the characteristics of pulsating flow are mainly governed by the time-averaged Dean number ($Re_{ta}\sqrt{(D_h/2R)}$), the dimensionless angular frequency($\omega^+$), and the velocity amplitude ratio ($A_1$).

### 3.3 Secondary flow

Figs 6 and 7 show the result of secondary flows according to variation along the z*-axis. The axis of the abscissa indicates a dimensionless value of the z-axis, and the axis of the ordinate indicates a dimensionless value of $V_{ps}/U_{m,ta}$, as shown in Fig. 2.

When the dimensionless angular frequency ($\omega^+$) is 18.2, secondary flow becomes complex because of an unsteady influence according to the increase in dimensionless angular frequency by the bending effect of the curved duct. Secondary flow profiles become relatively complex in the entrance region.

In Fig. 6 ($De_{ta}=780$, $A_1=0.9$), the behavior of the secondary flow becomes complex at the upper and lower walls of the duct in the entrance region. When '$\phi$' is 30° of the bend, strong secondary flows are generated at the center of duct.

Strong secondary flows are generated from the outer wall to the inner wall at 30° of bend angle when the phase angle ($\omega t/\pi/6$) is 0 or 6, but they are generated at 90° of bend angle only when the phase angle ($\omega t/\pi/6$) is 6.

As shown in Fig. 7, as $A_1$ decreases relatively, the viscosity force increases relative to the inertia force. Results showed a smaller amplitude than that of Fig. 6. Since the steady flow component becomes stronger than that of the

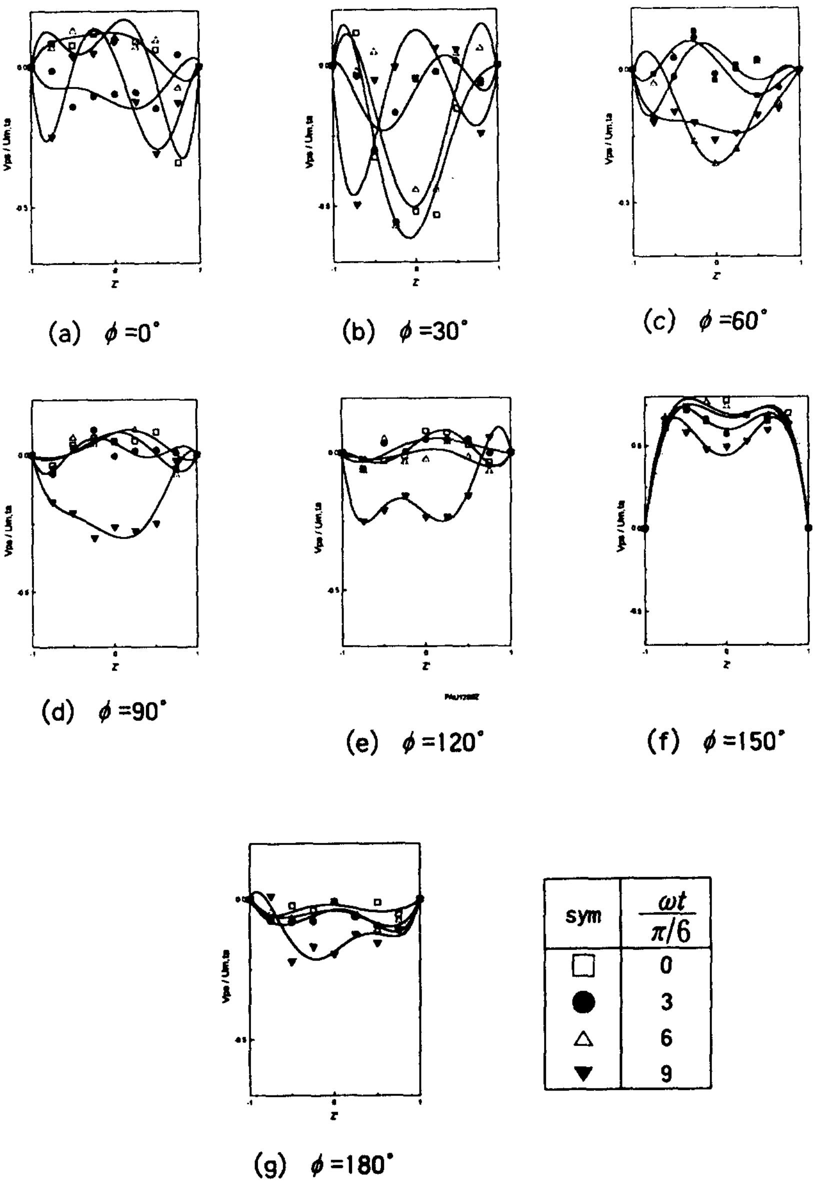


**Fig. 6 Secondary flow distributions along the z* variation in a curved duct for turbulent pulsating flow at $De_{ta}=780$, $\omega^+=18.2$, $A_1=0.9$.**

oscillatory flow, pulsating flow is similar to steady flow. A strong secondary flow is generated at 30° of bend in a turbulent pulsating flow.

### 3.4 Wall shear stress distribution

Wall shear stress distributions of dimensionless which any wall shear stress divided by maximum value of wall shear stress are represented in accordance with bend angle at 150° curved duct position. The axis of abscissa (ordinates) indicates a position of dimensionless value of $\tau_w/\tau_{w,max}$.

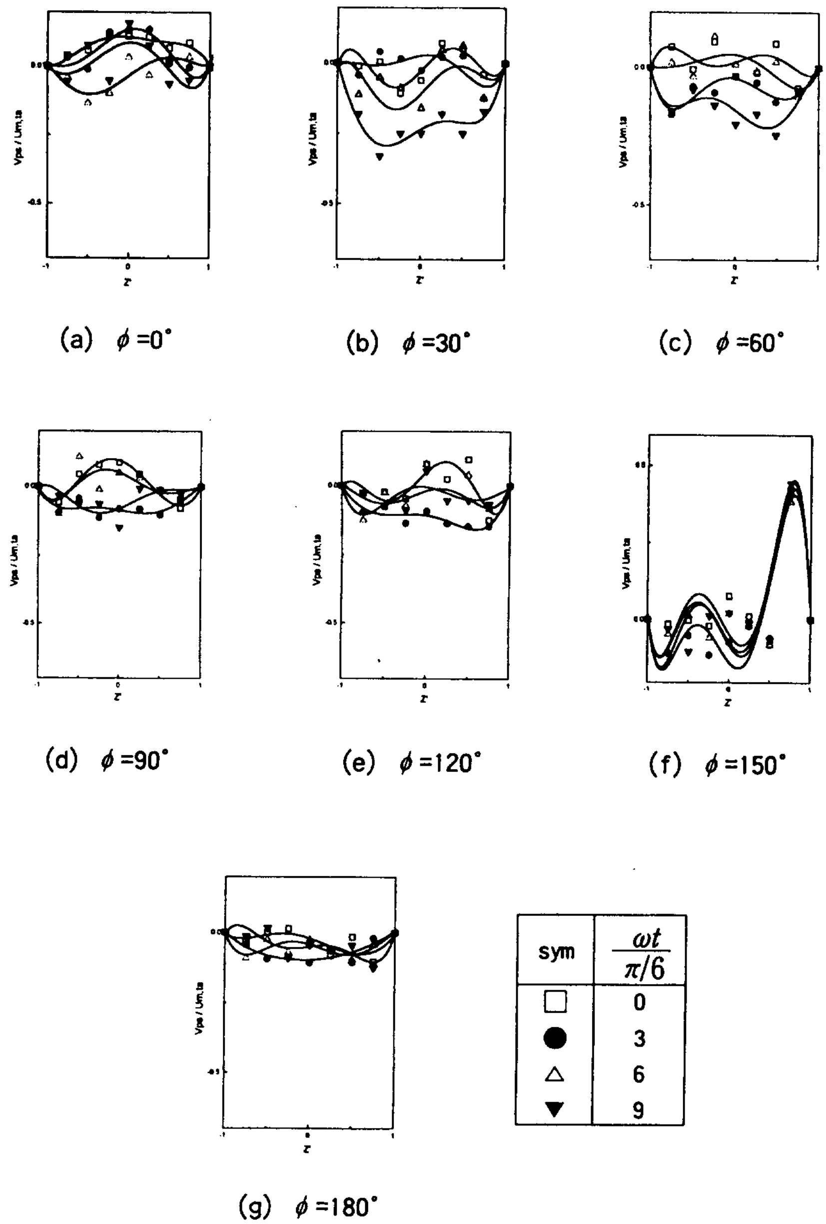


| sym | $\frac{\omega t}{\pi/6}$ |
|---|---|
| □ | 0 |
| ● | 3 |
| △ | 6 |
| ▼ | 9 |

**Fig. 7 Secondary flow distributions along the z* variation in a curved duct for turbulent pulsating flow at $De_{ta}=990$, $\omega'=18.2$, $A_1=0.7$.**

In Fig. 8, when the dimensionless angular frequency is small, the axial velocity generates a secondary flow, making the velocity gradient larger at the near wall. This indicates that flow in an oscillatory boundary layer is affected by secondary flow ; as a result, the velocity gradient has a gentle slope at the wall.

During one cycle, wall shear stress distributions become maximum at the outer wall. They decreased gradually as they moved to the cen-

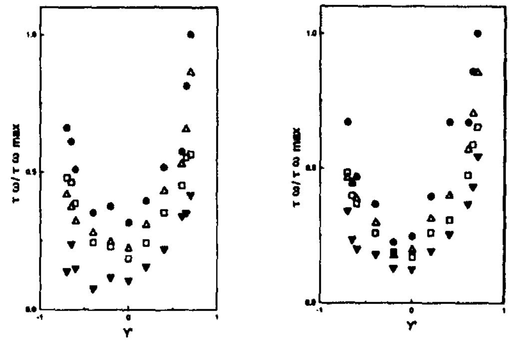

(a) (b)

**Fig. 8 Wall shear stress distributions for turbulent pulsating flow at $De_{ta}=780$, $\omega^{+}=18.2$, $A_1=0.9$ and $De_{ta}=990$, $\omega^{+}=18.2$, $A_1=0.7$.**

ter, where they reached a minimum. As '$A_1$' decreases, wall shear stress distributions show a constant value regardless of phase angle. It is this reason that the inertia force becomes weak and the viscous force becomes strong as a result of their unsteady nature.

## 4. Conclusions

In a square cross-sectional 180° curved duct, the conclusion, which is obtained from experimental study by using L.D.V. about transitional pulsating flow, is as follows ;

1. In a square-sectional curved duct, the critical Dean number($De_{pu,cr}$) changes a laminar pulsating flow into a transitional pulsating flow and is about $60\omega^{+}$. The critical Dean number($De_{pu,cr}$) changes a transitional pulsating flow into a turbulent pulsating flow and is greater than $75\omega^{+}$.

2. The velocity profiles of turbulent pulsating flow are similar to those of steady flow. If the velocity of dimensionless angular frequency increases, the axial velocity profiles do not change. The maximum velocity shifts to the outer wall under the influence of the centrifugal force at 30° of bend. Axial velocity energy and secondary velocity energy are balanced ; the main flow velocity is offset by the influence of secondary flow, and then the amplitude becomes small.

3. The secondary flow of turbulent pulsation is complex in the entrance region, while past the entrance secondary flow becomes strong from 30° of bend. As the velocity amplitude becomes larger, secondary flow becomes stronger and is strong in the entrance region.

4. If $A_1$ decreases, wall shear stress distributions show a gradual tendency toward a constant value regardless of phase angle. It is for this reason that the inertial force becomes a weak and viscous force becomes a strong by unsteady characteristics.

## Acknowledgement

'This study is supported by the academic research fund of the Ministry of Education, Republic of Korea.'

## REFERENCES

1. Eustice, J., "Flow of Water in Curved Pipes," Proc. R. Soc, Ser. A. 84-568, pp. 107~118, 1910.
2. Dean, W. R., "Note on the Motion of Fluid in a Curved Pipe," *Phil. Mag.* S. 7, Vol. 4, No. 20, pp. 208~223, 1927.
3. Lyne, W. H., "Unsteady Viscous Flow in a Curved Pipe," *J. Fluid Mech.* Vol. 45, Part. 1, pp. 13~31, 1970.
4. Zalosh, R. G., and Nelson, W. G., "Pulsating Flow in a Curved Tube," *J.Fluid Mech.* Vol. 59, Part 4, pp. 693~705, 1973.
5. Mullin, T., and Greated, C. A., "Oscillatory Flow in Curved Pipes. Part 2. The Fully Developed case," *J. Fluid Mech.* Vol. 98, part 2, pp. 397~416, 1980.
6. Smith, F. T., "Fluid Flow into a Curved Pipe", *Proc. R. Soc. Ser.* A. 351, pp. 71~87, 1976.

7. Singh, M. P., "Entry flow in a Curved Pipe ", *J. Fluid Mech*, Vol. 65, part. 3, pp. 517～539, 1974.
8. Singh, M.P., Sinha, P. C., and Meena Aggarwal, "Flow in the Entrance of the Aorta", *J. Fluid Mech*, Vol. 87, part. 1, pp. 97～120, 1978.
9. Talbot, L., and Gong, K. O., "Pulsatile Entrance Flow in a Curved Pipe", *J. Fluid Mech*, Vol. 127, pp. 1～25, 1983.
10. Kita, Y., Korou, R., Hirose, K., and Nakano, A., "Turbulent Flow in a Curved Duct with a Rectangular Cross-Section (6th Report, Flow in Entrance Region in Pulsatile Flow)", *J. Fluid Mech*, Vol. 55, No. 511, pp. 585～591, 1989.
11. Naruse, T., Nishina, Y., Ishihara, K., Tanishita, K., "内頸動脈における拍動流推移", *J. Fluid Mech*. Vol. 57, No. 541, pp. 3018～3025, 1991.
12. Sumida, M., and Sudou, K., "Pulsating Flow in Curved Pipes (5th Report, Velocity Distribution in Entrance Region)", *J. Fluid Mech*, Vol. 61, No. 587, pp. 2442～2449, 1995.
13. Austin, L.R., and Seader, J. D., "Fully Developed Viscous Flow in Coiled Circular Pipes", AICHE. J., Vol. 19, No. 1, pp. 85～93, 1973.

## 저 자 소 개

**박길문(朴吉文)**

1949년 3월생. 1974년 조선대학교 기계공학과 졸업. 1977년 고려대학교 대학원 기계공학과 졸업(석사). 1987년 동 대학원 기계공학과 졸업(박사). 1978년～현재 조선대학교 기계공학과 교수.

**봉태근(奉部根)**

1956년 3월생. 1978년 목포해양대학교 기관학과 졸업. 1989년 조선대학교 대학원 기계공학과 졸업(석사). 1997년 동 대학원 기계공학과 졸업(박사). 1982～현재 목포해양대학교 기관공학부 조교수. 당학회 종신회원

**손현철(孫鉉澈)**

1965년 9월생. 1990년 금오공과대학교 기계공학과 졸업. 1994년 동 대학원 기계공학과 졸업(석사). 1999년 조선대학교 대학원 기계공학과 수료(박사).